Application of computational fluid dynamics for the analysis of the furnace effect in the determination of the temperature of high temperature fixed points \odot

Pablo Castro

; Cesar del Pozo; Graham Machin

AIP Conf. Proc. 3230, 070007 (2024) https://doi.org/10.1063/5.0234115





Articles You May Be Interested In

High-temperature fixed-point furnace uncertainties

AIP Conf. Proc. (October 2024)

Realizing Fe-C, Pd-C, Ru-C and WC-C eutectic fixed-points at UME

AIP Conf. Proc. (October 2024)

Research on aluminum-based eutectic fixed-point cells in portable dry-body thermostat

AIP Conf. Proc. (October 2024)

Challenge us.

What are your needs for periodic signal detection?



Find out more





Application of Computational Fluid Dynamics for the Analysis of the Furnace Effect in the Determination of the Temperature of High Temperature Fixed Points

Pablo Castro^{1, a)}, Cesar del Pozo^{1, b)}, and Graham Machin^{2, c)}

¹Universidad de Cantabria, Avda. Los Castros s/n, 39005, Santander, Spain ²National Physical Laboratory, Hampton Rd., Teddington, Middlesex, TW11 0LW, UK

^{a)}Corresponding author: pablo.castro@unican.es ^{b)}cesar.del-pozo@alumnos.unican.es ^{c)}graham.machin@npl.co.uk

Abstract. High-temperature fixed-points (HTFPs) have been intensely studied in the last two decades. Yet despite this there are still sources of poorly characterized uncertainty one of which is colloquially known as the "furnace effect". This has been attributed to different factors, examples of which include: the lack of uniformity of the furnace temperature, the thermal inertia of the furnace, the microstructure of the fixed point material, the heat dissipation through the walls of the furnace and cell, the effective emissivity of the black body cavity and the characteristics of the radiation thermometer. However, it has been shown that, all of these are too small to explain the magnitude of the temperature drop obtained and more recent research has indicated that this uncertainty is related to the specific configuration of the furnace and cell considered, so purely a geometric phenomenon.

In that work it was shown that the furnace effect was caused by the interaction between the thermal radiation from the hot furnace tube and the inside of the blackbody cavity, specifically due to the reflection of the furnace thermal radiation from the HTFP cavity sidewall. To demonstrate this several modifications were made to a specially designed Cu fixed-point blackbody, these were; a means of reducing the diameter of the blackbody aperture, incorporation of radiation shield disks and making circumferential grooves on the inner surface of the HTFP blackbody. These modifications reduced the furnace effect for the copper fixed point by around 14 mK.

The aim of this paper is to apply Computational Fluid Dynamics (CFD) to the analysis of the furnace effect to better understand its mechanism and to assess how much each mitigation strategy contributes to reducing the furnace effect. The results obtained using ANSYS[©], have confirmed that the introduction of appropriate improvements in the black body cavity design reduces the magnitude of the furnace effect and that the most influential factor is the reduction of the cell aperture diameter, which, incidentally, confirms that this phenomenon is mainly caused by the reflected thermal radiation from the cavity sidewall.

Here it was not possible to determine realistic values for the furnace effect, mainly due to the complexity of considering the variation of the specular component of the reflectance as a function of the angle of incidence of the irradiance, nevertheless qualitative results are in line with the observations.

INTRODUCTION

High Temperature Fixed Points (HTFPs) [1] have been the subject of intensive research for more than two decades leading to their acceptance as ultra-reliable references for high temperature measurement. One of the minor issues concerning their operation is a source of uncertainty colloquially known as the furnace effect [2]. The origin of this effect has been the subject of considerable speculation but recent work reported by Yamada [3] gave tantalizing indications as to its source.

Previous studies carried out by [4] to verify the existence of the furnace effect using a copper fixed point identify uncertainties in the temperature of up to 120 mK, which could not be explained by the effect of the radiation thermometer Size of Source Effect (SSE), or for any other obvious cause.

More recently research into the furnace effect [5] was carried using the HTFP of Co-C (1597 K), using two different types of crucibles but with similar designs and three types of furnaces (tubular C / C indirect heating, tubular graphite direct heating and alumina tube indirect heating). In this case, uncertainties in the measurement were up to 140 mK.

Different attempts have been made to explain the source of the furnace effect: the lack of uniformity of the furnace temperature [6], the thermal inertia of the furnace [7], the ingot microstructure of the fixed point material used or the emissivity of the cavity and the SSE [5], the temperature drop through the walls of the cavity [8]. However, these phenomena are too small, even as a whole, to explain the magnitude of the temperature drop experienced when the measurement is made [3].

For this reason research was performed [9] to try to identify the real cause of the furnace effect, using a copper fixed point blackbody. In this research, three types of furnace with different design, dimension and heating principle (tubular C/C indirect heating, compact indirect heating and three zones furnace with indirect heating alumina tube), two types of crucibles with different designs and dimensions, and two radiation thermometers with different wavelengths and different value of the SSE were used.

The results of this study showed that the furnace effect depended on the length of the furnace tube and the design of the crucible. However, no clear relationship was found between the dimensions of the crucible and the furnace effect, nor a dependence associated with the radiation thermometer used [3, 9].

Finally, in the research carried out by [3], the same types of furnace and crucible designs were used, and copper was used as the fixed-point but only a radiation thermometer with a small SSE was used. This study was a continuation of the previous research [9], but this time investigated the effect of different crucible aperture diameter and a series of discs acting as radiation shields in front of the crucible.

The results obtained verified that the modifications introduced in the design of the crucible reduced the furnace effect, confirming that this phenomenon was caused by the interaction of the radiant energy from the furnace wall in front of the crucible with the interior cavity of the furnace. The paper goes on to suggest that the furnace effect was mainly due to reflection of the radiation (from the furnace-tube) by the side wall of that cavity. This was strongly suggested by the results because when the crucible aperture was reduced, the observed furnace effect was significantly reduced to 14 mK [3].

Here we establish a CFD model of the crucible-furnace configuration which allows us to investigate the effect of changing different key parameters, such as crucible aperture, relating to the furnace and the crucible and materials properties such as graphite emissivity. We report on the results of that modelling and discuss them in the light of the reported experimental data regarding the source of the furnace effect.

MODEL DESIGN DESCRIPTION

The different configurations of furnace and crucible considered in the analysis of the furnace effect with $ANSYS^{\odot}$ were based on:

- A Nagano furnace (VR10 A45): manufactured by Nagano Co., Ltd. It is composed of a C/C tube 250 mm long and 27 mm in internal diameter, closed at one end, inside which the crucible is housed. In addition, the Nagano furnace has a series of discs distributed equidistantly along the inside of the furnace tube, which serve as thermal radiation shields.
- S-type crucible: this is the smallest type of crucible and the one with the most conventional design for this class of tests. It is installed inside the Nagano furnace and made of high purity graphite.

From this furnace-cell configuration, 4 different cases were designed, with the dimensions shown in Figure 1 and where differences between configurations are only the aperture area of the cell and the length of the hot furnace tube:

- Case I: 3 mm cell aperture diameter and 48 mm tube length beyond the blackbody aperture.
- Case II: 3 mm cell aperture diameter and 72 mm tube length beyond the blackbody aperture.
- Case III: 1.5 mm cell aperture diameter and 48 mm tube length beyond the blackbody aperture.
- Case IV: 1.5 mm cell aperture diameter and 72 mm tube length beyond the blackbody aperture.

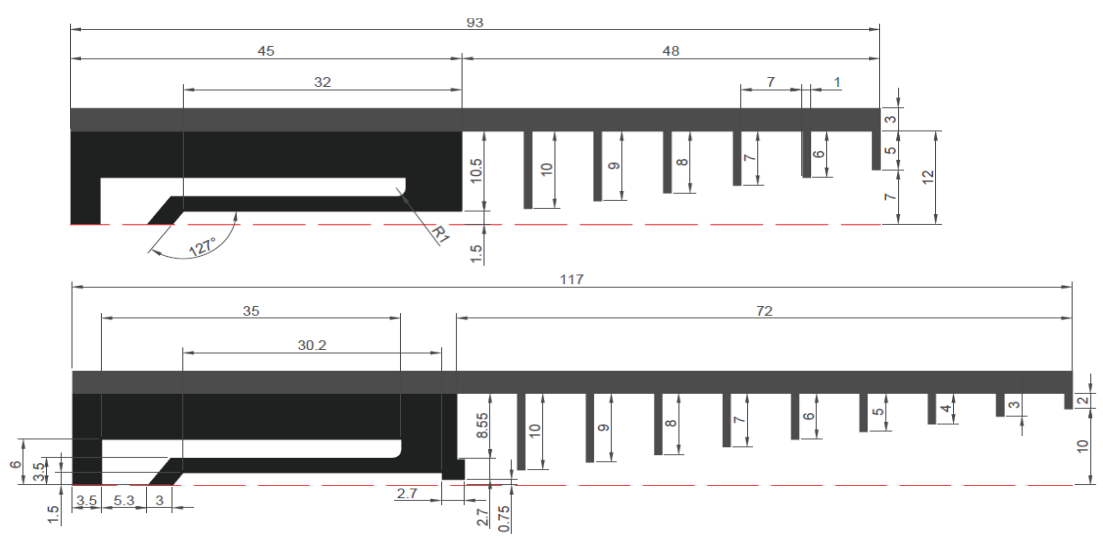


FIGURE 1. Dimensions (in mm) for the two cell aperture diameters and the two tube lengths beyond the blackbody aperture

A total of 6 discs distributed equidistantly along the entire length of the furnace tube were included in cases of 48 mm, while 9 discs were placed in the cases of 72 mm, as can be seen in Figure 2.

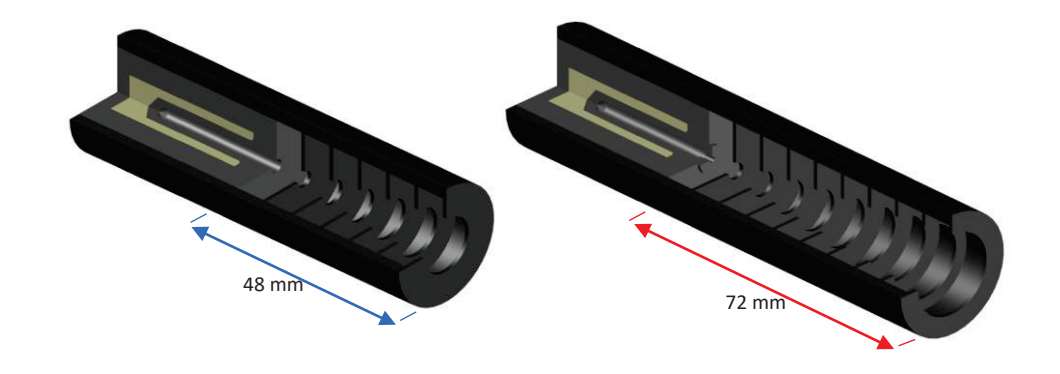


FIGURE 2. Representation of the radiation shields placed along the tube beyond the blackbody aperture

The fixed-point materials which were modelled were; Copper (Cu, 1358 K), Cobalt Carbon (Co-C, 1597 K), Platinum-Carbon (Pt-C, 2011 K) and Rhenium-Carbon (Re-C, 2747 K).

RESULTS

In the simulations the graphite surface emissivity (ϵ) ranged from 0.85 to 0.95 and the diffuse fraction (DF), that is the portion of the reflectivity considered diffuse, varied from 0.5 to 1 for the side wall of the cavity of the blackbody to simulate the specular reflectivity for low angles detected in [3].

The main results are summarized in Tables 1, 2, 3 and 4, one for each case studied.

TABLE 1. Backwall temperature drop for case I with emissivity and diffuse fraction variation.

Backwall temperature drop / mK			Cu		Со-С			Pt-C			Re-C			
		Emissivity			Emissivity			Emissivity			Emissivity			
		0.85	0.9	0.95	0.85	0.9	0.95	0.85	0.9	0.95	0.85	0.9	0.95	
Diffuse fraction	0.5	4.8	4.2	3.6	9.0	7.9	6.6	22.4	19.5	16.3	77.0	66.9	55.9	
	0.75	3.7	3.5	3.2	7.0	6.5	5.9	17.2	15.9	14.5	58.8	54.4	49.5	
	1	2.6	2.7	2.8	4.9	5.0	5.2	11.9	12.3	12.6	40.8	41.9	43.1	

TABLE 2. Backwall temperature drop for case II with emissivity and diffuse fraction variation.

Backwall temperature drop / mK			Cu		Со-С				Re-C				
		Emissivity			Emissivity				Emissivity				
		0.85	0.9	0.95	0.85	0.9	0.95	0.85	0.9	0.95	0.85	0.9	0.95
Diffuse fraction	0.5	4.7	4.1	3.4	8.8	7.7	6.4	21.7	18.9	15.8	74,5	64.7	53.9
	0.75	3.6	3.4	3.1	6.8	6.3	5.7	16.6	15.4	14.0	56.9	52.4	47.6
	1	2.6	2.6	2.7	4.7	4.8	5.0	11.5	11.8	12.1	39.2	40.2	41.3

TABLE 3. Backwall temperature drop for case III with emissivity and diffuse fraction variation.

Backwall temperature drop / mK			Cu			Со-С		Pt-C			Re-C		
		Emissivity			Emissivity			l	Emissivit	Emissivity			
		0.85	0.9	0.95	0.85	0.9	0.95	0.85	0.9	0.95	0.85	0.9	0.95
Diffuse fraction	0.5	1.4	1.2	1.1	2.5	2.2	1.9	5.8	5.1	4.4	19.2	16.8	14.3
	0.75	1.2	1.1	1.0	2.0	1.9	1.7	4.5	4.2	3.9	14.8	13.9	12.8
	1	0.9	0.9	0.9	1.5	1.5	1.6	3.3	3.4	3.5	10.5	10.9	11.2

TABLE 4. Backwall temperature drop for case IV with emissivity and diffuse fraction variation.

Backwall temperature drop / mK		Cu Emissivity				Со-С		Pt-C			Re-C		
					Emissivity			Emissivity			Emissivity		
		0.85	0.9	0.95	0.85	0.9	0.95	0.85	0.9	0.95	0.85	0.9	0.95
e n	0.5	1.3	1.1	1.1	2.4	2.2	1.9	5.7	5.0	4.3	18.8	16.5	13.9
Diffuse fraction	0.75	1.1	1.1	1.0	2.0	1.8	1.7	4.5	4.2	3.9	14.5	13.5	12.4
	1	0.9	0.9	0.9	1.5	1.5	1.5	3.2	3.3	3.4	10.2	10.5	10.9

Figure 3 represents the variation of the backwall temperature drop for the 4 configurations and the 4 HTFP all with emissivity value of 0.9 and diffuse fraction of 0.75.

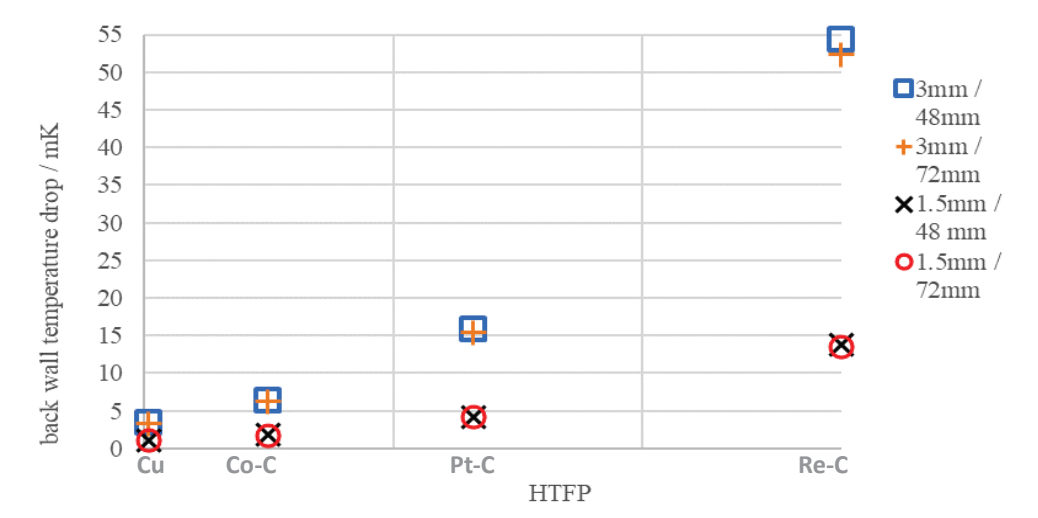


FIGURE 3. Backwall temperature drop with cell aperture diameter and furnace tube length beyond blackbody aperture. Data for ϵ =0.9 and DF=0.75

DISCUSSION

From the results it is clear that for a given value of the diffuse fraction, the higher the emissivity of the inside surfaces of the cavity, the lower the temperature drop experienced in the backwall. That is the cavity more closely approximates to an ideal blackbody.

In addition for a given emissivity value, the higher the diffuse fraction, the lower the temperature drop experienced on the backwall. This is because the higher the DF value, that is, the proportion of radiant energy that is emitted and/or reflected diffusely, the lower the part of that energy that will be reflected specularly, so there will be a greater number of interactions between the radiant energy and the inner walls of the cavity of the furnace-crucible assembly, which translates into a lower heat loss by thermal radiation to the outside.

Therefore, analyzing both behaviours together, it is possible to affirm that the higher the emissivity and the diffuse fraction of the graphite surfaces involved, the lower the temperature drop in the backwall, and *vice versa*. This is true for all furnace-cell geometries and for all fixed-point materials considered. This is physically intuitive and confirms that the model can at least qualitatively predict the contributing factors to the furnace effect.

When seeking to identify the contribution of key factors to mitigate the furnace effect two modifications were introduced into the geometry of the furnace-cell model under study. From these the following is observed:

For the same blackbody aperture diameter (d), the temperature drop experienced in the backwall is lower the longer the furnace tube length beyond blackbody aperture (L). When considering a furnace geometry with a tube length of L=72 mm, the temperature drop in the backwall, assuming the same conditions of emissivity and diffuse fraction and regardless of the fixed-point material used, was around 3% lower than using a furnace-cell geometry with the same value of d, but with an L=48 mm. Hence in this situation the furnace length had a very modest effect on furnace effect.

However, when considering a value of d=1.5 mm, the temperature drop in the backwall for the same conditions of emissivity and diffuse fraction and regardless of the fixed point material used, was around 70% lower than in the case of using a furnace-cell geometry with the same value of L, but with d=3 mm.

It is clear that the impact on the backwall temperature drop and, therefore on the furnace effect, caused by the reduction of the cell aperture diameter, is much higher than that due to the increase in the length of the furnace tube beyond the blackbody cavity and the number of radiation shielding discs. This confirms the fact that the furnace effect mainly arises from the reflection of radiant energy from the side wall of the inner cavity of the crucible. This indicates that blackbody aperture, smaller than the actual blackbody tube diameter, is a key factor in mitigating furnace effect.

Finally, when comparing the measurement results [3] corresponding to the simulations carried out for the copper fixed point (1.5 mm aperture) [1], a significant difference is observed. While in these simulations the backwall temperature drop varied in the range 0.9-1.3 mK depending on the values of ϵ and DF considered, in the measurements [3] this drop has reached a value around 14 mK.

This difference possibly point to the need of a more sophisticated specular – diffuse model, which would be able to capture with greater precision the relationship between the angle of incidence of the radiated energy and the specular component of the reflectance. Other possible causes outside the furnace effect that could be distorting its value should be explored, such as those due to heat dissipation by conduction and convection to the environment, the characteristics of the radiation thermometer or the presence of a temperature gradient inside the furnace.

CONCLUSIONS

An increase in the furnace tube length beyond blackbody aperture of 33% (24 mm), achieves a small improvement in the blackbody temperature drop of around 3%, which translates into a reduction of the furnace effect of approximately 0.2% for each millimeter of increase in tube length, regardless of the fixed-point material used. A reduction of the crucible aperture diameter of 50% (1.5 mm), obtains an improvement in the backwall temperature drop of around 70%, which translates into a reduction of the furnace effect of approximately 48% per millimeter of reduction of the crucible aperture diameter, regardless of the fixed point material considered.

On the one hand, the fact that the reduction of the cell aperture diameter presents a much greater impact on the reduction of the furnace effect than the increase in the furnace tube length, confirms that this effect is very sensitive to the reflected thermal radiation from the side wall of the inner cavity of the crucible. On the other hand, the higher the value of the emissivity (ϵ) and/or the diffuse fraction (DF) of the graphite surfaces inside the cavity of the furnace-crucible assembly, the lower the value of the temperature drop obtained in the backwall.

Therefore, the most influential factors on the furnace effect are, in order of importance:

- a) The diameter of the HTFP blackbody aperture.
- b) The specularity of wall of the HTFP blackbody.
- c) Surface emissivity of the graphite.

These results can be used to guide future designs of HTFP/furnace configuration to minimise the furnace effect. The furnace effect values found here are lower than those reported in the literature; possibly due to overly optimistic assumptions about the graphite emissivity and too conservative diffuse fraction. Other reasons for the smaller values, which were not taken into account in the modelling, could be:

- The dissipation of heat by convection through the furnace aperture to the outside by the presence of a flow of argon gas inside the cavity.
- The presence of a temperature gradient inside the furnace.
- The characteristics of the radiation thermometer used.
- The need for a more sophisticated specular diffuse model, which more reliably simulated the relationship between the angle of incidence of the irradiated energy and the specular component of the reflectance.

REFERENCES

- 1. G. Machin, AIP Conf. Proc., 1552, 305 (2013); https://doi.org/10.1063/1.4821383
- 2. A. Todd, et al, Metrologia 58 035007 (8pp) (2021) https://doi.org/10.1088/1681-7575/abe9c5
- 3. Y. Yamada, *Meas. Sci. & Technol.* **32** 015009 (2020) https://doi.org/10.1088/1361-6501/abafe2
- 4. A. Todd & D. Woods, *Int. J. Thermophys.*, **35**, 1377. (2014) https://doi.org/10.1007/s10765-014-1666-5
- 5. W. Dong, et al. Measurement, 106, pp. 88–94. (2017) https://doi.org/10.1016/j.measurement.2017.04.005
- F. Bourson, et al. AIP Conf. Proc., 1552(1), 380 (2013) https://doi.org/10.1063/1.4821389
- 7. P. Bloembergen, et al, Int. J. Thermophys., 36, 1859 (2015) https://blodoi.org/10.1007/s10765-015-1892-5
- 8. D. Lowe, Meas. Sci. & Technol. 24(1), 015901. (2013) https://doi.org/10.1088/0957-0233/24/1/015901
- 9. M. Imbe & Y. Yamada, *Meas. Sci. & Technol.* **27**(12), 125020. (2016) https://doi.org/10.1088/0957-0233/27/12/125020